DELINEATION OF VEGETATION AND BUILDING POLYGONS FROM FULL-WAVEFORM AIRBORNE LIDAR DATA USING OPALS SOFTWARE

M. Hollaus*, W. Wagner, G. Molnar, G. Mandlburger, C. Nothegger, J. Otepka

Institute of Photogrammetry and Remote Sensing, Vienna University of Technology,
Gußhausstraße 27-29, 1040 Vienna, Austria - mh(ww, gmo, gm, jo)@ipf.tuwien.ac.at

KEY WORDS: Three-dimensional, LIDAR, Retrieval, Roughness, Land Cover, Full-Waveform

ABSTRACT:

Full-waveform LiDAR is an active remote sensing technique that provides the scattering properties of the targets i.e. amplitude and echo width (EW) in addition to 3D point clouds. The amplitude provides information on the target's reflectance and the EW is a measure for the range variation of scatterers within the laser footprint contributing to a single echo and is, therefore, an indicator for surface roughness. For the delineation of high vegetation (i.e. trees and bushes) and buildings the normalized digital surface model provides the main input. Based on a height threshold, areas covered with elevated objects can be classified. For the differentiation between buildings and high vegetation the surface roughness is used, where roofs are assumed to be smooth and vegetation rough. The surface roughness can be described with the standard deviation (SD) of detrended LiDAR points. However, for low LiDAR point densities and for very dense deciduous forests or building parts overgrown with tree crowns the separability is limited if only the SD is used. Within the presented approach additionally the EW, featuring small values for smooth roof areas, and the echo ratio (ER), a measure for the penetrability of a surface, are used. For the final delineation of high vegetation and building areas morphologic operations are applied. The classified areas are vectorized and a minimum mapping unit is applied. The presented workflow is implemented into the scientific software package OPALS (Orientation and Processing of Airborne Laser Scanning data). The results show that the EW, the SD and the ER are useful quantities to delineate high vegetation and building polygons based on full-waveform LiDAR point clouds with high accuracy. The high degree of automation and the scripting capability OPALS promise a high potential for operational large area LiDAR data processing. Examples from different test sites in Austria are shown and discussed.

1. INTRODUCTION

The detection of buildings and vegetation (i.e. trees and bushes), which is an important part of land cover classifications, has a long history in remote sensing applications. Miller and Small (2003) give an extensive review of studies highlighting potential applications of remote sensing for urban environments. As the dynamic of urban landscapes causes increasing problems in terms of competing land use, private transport, infrastructure costs and environmental aspects the demand on reliable techniques and tools to monitor, describe and evaluate these developments increases. For example up-to-date spatial data sources are the basis for modeling noise and pollution mitigation.

Traditionally, different multi-spectral images (e.g. satellite images, aerial photographs) with different spatial resolutions (e.g. 0.25 m to 30.0 m) are in use to derive these land cover classes based on pixel- or object-based classification approaches. However, these data sources are mainly used to derive 2D information and therefore, attributes such as building and vegetation heights are not available for the classification, which limits for example the differentiation between objects with similar spectral and textural characteristics e.g. streets and roofs that can both be built of similar materials. A major step towards an increase of the accuracy of urban land cover from remotely sensed data was the involvement of object heights above the terrain surface. For example, Haala and Walter (1999) used local height information derived from airborne LiDAR data in combination with multi-spectral imagery to separate buildings, trees, streets and grass-covered areas within an urban environment.

One of the most promising approaches to derive object heights is the usage of airborne LiDAR data, which has been established as a standard data source for the generation of high precision digital terrain models (DTM) during the last decade. The LiDAR technology has several advantages comparing to stereoscopic analysis of aerial images. ALS systems are active remote sensing systems and are characterized by a simple measurement geometry, i.e. the 3D-position of an object point on the surface is measured from a single location. Thus, also for densely built-up areas with small streets precise topographic models can be generated and building as well as vegetation models can be determined performantly. The newest generation of LiDAR sensors digitizing the full-waveform of the backscattered signal provides the scattering properties of the targets i.e. amplitude and echo width (EW) in addition to the 3D point cloud. The amplitude supplies information on the target's reflectance and the EW is a measure for the range variation of scatterers within the laser footprint contributing to a single echo and is, therefore, an indicator for surface roughness, which is useable for separating roof and canopy surfaces (Rottensteiner et al., 2005).

The objectives of this paper are to show the benefits of additional quantities derived from full-waveform LiDAR data for the classification of buildings and high vegetation. The developed workflow was implemented with the - the scientific software

package OPALS (Orientation and Processing of Airborne Laser Scanning data) and was applied for different study areas in Austria.
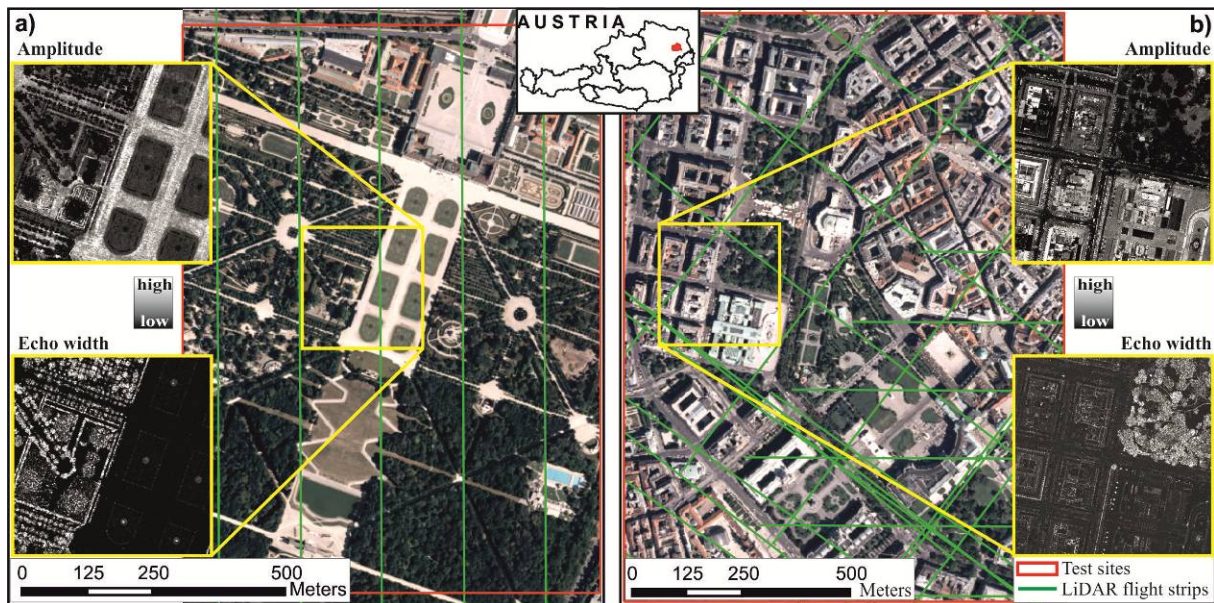

Figure 1. Overview of the study areas in the city of Vienna. (a) *Schönbrunn* test site and (b) *city centre* test site. Shown are aerial photographs superimposed with the trajectories of the LiDAR flight strips. Furthermore, the LiDAR echo widths and amplitudes are shown. All images have a spatial resolution of 0.5 m.

2. STUDY AREAS AND LIDAR DATA

2.1 Study areas

The proposed work flow for deriving vegetation and building outlines is applied for different test sites located in the city of Vienna, Austria. The first test site covers the *Schönbrunn* area whereas the second one is located in the city center. Fig. 1 gives an overview of the study areas.

The *Schönbrunn* test site has an area of 0.80 km x 1.08 km and covers the Schönbrunn Palace, the park area as well as the surrounding build-up areas. The city center test site has an area of 1.00 km x 1.35 km and covers three city parks (Rathauspark, Burggarten, Volksgarten) and the adjoining densely build-up areas. The parks are dominated by deciduous trees, but also coniferous trees, shrubs, park fences, walls and walking paths are available. The build-up areas are dominated by large buildings, streets, different types of parked vehicles, street lamps, overhead wires used by trams, etc.

3. DATA

For the entire city of Vienna full-waveform LiDAR data are available, which were acquired in the framework of a commercial terrain mapping project. The data acquisition was carried out under leaf-off conditions during the winter and spring season 2006/2007. The data were acquired by the company *Diamond Airborne Sensing GmbH*[1] in cooperation with *AREA Vermessung ZT GmbH*[2] using a *Riegl* LMS-Q560 laser scanner. This sensor uses short laser pulses with a wavelength of 1.5 μm and a pulse width of 4 ns. The laser beam divergence is 0.5 mrad and the scan angle varies between ±22.5°. The crosswise overlap of the flight strips were approx. 50%. The average flight altitude was about 500 m above ground, which resulted in an average laser footprint diameter of 0.25 m on the ground. The average point density is 20 echoes per square meter. The trajectories of the individual flight strips are shown in Fig. 1. The pre-processing of the FWF-ALS data (i.e. Gaussian decomposition, strip adjustment, georeferencing) was done by the company *AREA Vermessung ZT GmbH* using the *RIEGL* software packages[3].

The applied Gaussian decomposition of the backscattered waveforms is based on the fact that the system waveform of the *RIEGL* LMS-Q560 is well described by a Gaussian function and consequently the received backscattered waveform is a result of a convolution of the system waveform and the differential cross-section of the illuminated object surface (Wagner et al., 2006). As a result of the Gaussian decomposition, several targets can be modeled within a complex waveform and for each detectable echo the range, the amplitude, and the echo width are obtained. Due to the short laser pulse duration of the LMS-Q560 (τ = 4 ns)

---

[1] http://www.diamond-air.at/airbornesensing.html

[2] http://www.area-vermessung.at/

[3] http://www.riegl.com/nc/products/airborne-scanning/

A special joint symposium of ISPRS Technical Commission IV & AutoCarto
in conjunction with
ASPRS/CaGIS 2010 Fall Specialty Conference
November 15-19, 2010 Orlando, Florida

scattering targets, separated by a minimum distance of 0.6 m can be differentiated.

For the current study the geo-referenced 3D echo points and the determined attributes for each echo, i.e. the echo width and the amplitude, were provided by the city administration of Vienna (*MA41-Stadtvermessung*). Images of the amplitudes and the EWs, calculated based on the highest points within raster cells with a spatial resolution of 0.25 m, are shown in Fig. 1. The digital terrain model (DTM) was calculated using the SCOP++ (2010) software. For the determination of the digital surface model (DSM) the approach described in Hollaus et al. (2010) was applied using the OPALS (2010) software. Further details about the DSM generation are given in the following sections. The derived DTM has a spatial resolution of 0.5 m.

4. Methods

4.1 Overview of the Workflow

For the delineation of high vegetation (i.e. trees and bushes) and buildings the normalized digital surface model (nDSM) provides the main input. Based on a height threshold, areas covered with elevated objects can be classified. For the differentiation between buildings and high vegetation the surface roughness is used. Thereby, roofs are assumed to be smooth and, whereas vegetation is rough. The roughness can be described by the standard deviation (σ_z) of the detrended LiDAR points. However, for low LiDAR point densities and for very dense deciduous forests or building parts overgrown with tree crowns the separability is limited if only σ_z is used. Therefore, within the presented approach additional parameters are used, namely, the EW and the slope adaptive echo ratio (sER). Both parameters provide local roughness measures. A knowledge-based decision tree is used for the classification of building and vegetation areas. The thresholds for the individual input data are assessed empirically. For the final delineation of high vegetation and building areas morphologic operations are applied. The classified areas are vectorized and a minimum mapping unit is applied for each class. The presented workflow is implemented with the scientific software package OPALS (**O**rientation and **P**rocessing of **A**irborne **L**aser **S**canning data).

4.2 nDSM Calculatioin

For the calculation of the DSM and, consequently, of the nDSM the land cover dependent approach for deriving DSMs from LiDAR data as descibed in Hollaus et al. (2010) was used. Depending on the surface roughness the surface model determined from the highest point within a defined raster cell (DSM_{max}) or the surface model based on moving least squares interpolation e.g. moving planes (DSM_{mls}) is used. Especially for low LiDAR point densities void pixels can occur in the DSM_{max} and for inclined smooth surfaces the DSM_{max} shows an artificial roughness mainly due to the irregular point distribution. On the other hand, the DSM_{mls} introduces smoothing effects along surface discontinuities e.g. building borders, tree tops or forest gaps. Therefore, the used approach makes use of the strengths of both DSMs and combines pixels from DSM_{mls} for smooth surface

parts and in case of void DSM_{max} pixels and DSM_{max} pixels otherwise. As roughness indicator the standard error of the estimated grid post elevation (σ_z) is used, which is derived during the DSM_{mls} computation. Finally, the nDSM is calculated for both test sites by subtracting the DTMs from the combined DSMs. The derived topographic models (DSM and nDSM) have a spatial resolution of 0.5 m.

4.3 Slope adaptive Echo Ratio

As shown in previous studies (Höfle et al., 2009; Rutzinger et al., 2008) the slope adaptive echo ratio (sER) is a measure to describe surface roughness and is an indicator for the penetrability of a surface. The *sER* is defined as the ratio between the number of neighboring echoes in a fixed search distance (e.g. 1.0 m) measured in 3D (a sphere) and all echoes located within the same search distance in 2D (a vertical cylinder) (Höfle et al., 2009; Rutzinger et al., 2008). An sER value of 100% means that the echoes within the 2D search radius describe a continuous and un-penetrable surface (e.g. roofs, roads), whereas a sER value <100% means that the echoes are vertically distributed within the 2D search area and, thus, indicating transparent objects i.e. forests, building borders and power lines.

4.4 Standard deviation of detrented LiDAR points

For describing the surface roughness the standard deviation (σ_z) of the detrended z-coordinates of LiDAR echoes within a raster cell or a certain distance of e.g. 1.0 m is used. For the calculation of σ_z all LiDAR echoes that are located near the surface (e.g. highest echoes within a raster cell of 0.5 m) are used. The detrending of the heights is important for slanted surfaces, where else the computed standard deviation would increase with increasing slope (i.e. height variation), even though the surface is plane. Therefore, the standard deviation of orthogonal regression plane fitting residuals is chosen. The orthogonal regression plane fitting is favored over vertical fitting because for very steep surfaces the vertical residuals can become very large, even though the plane fits very well to the points. In practical, for every laser echo the orthogonal plane fitting is performed in a local neighborhood (i.e. considering all terrain echo neighbors in a certain distance for plane computation; e.g. <1.0 m) and stored as additional attribute to the original laser echo. Further details about the surface roughness description based on LiDAR data can for example be found in Hollaus and Höfle (2010).

4.5 Echo width

As the echo width (EW) is a measure for the range variation of scattering objects within the laser footprint contributing to a single echo it is an indicator for surface roughness. For the presented approach EW is used for separating roof and canopy surfaces. Therefore, the highest LiDAR echoes within a pre-defined raster cell (e.g. 0.5 m cell size) are used to compute an EW-image (see Fig. 1).

A special joint symposium of ISPRS Technical Commission IV & AutoCarto
in conjunction with
ASPRS/CaGIS 2010 Fall Specialty Conference
November 15-19, 2010 Orlando, Florida

5. IMPLEMENTATION INTO OPALS

5.1 OPALS framework and data manager

OPALS (Mandlburger et al., 2009) is a scientific, modular software system consisting of small components (modules). The aim of OPALS is to provide a complete processing chain for processing airborne LiDAR data (waveform decomposition, georeferencing, quality control, structure line extraction, point cloud classification, DTM generation and several fields of application like forestry, hydrology/hydraulic engineering, city modeling and power lines). Each module is available as (i) a command line program, (ii) a Python module, and (iii) a C++ class (via DLL linkage). Complex workflows can be constructed by freely combining OPALS modules in a scripting environment (i.e., shell scripts or Python scripts). An efficient management of point cloud data is regarded to be of crucial importance. Thus, a central data administration unit (OPALS Data Manager, ODM) was developed. For spatial indexing of the point cloud, a two-level strategy is applied. First, the whole data set is organized in rectangular tiles and, secondly, for each tile a kd-tree is built up allowing high performance spatial queries. In contrast, all line related objects are stored in an R*-tree. Apart from a complete processing chain, another main goal of OPALS is to shorten the time span for transforming research results into software modules. This is mainly achieved by using a light-weight framework dealing with general programming issues like validation of user inputs, error handling, logging, etc. This allows non expert programmers to concentrate on the actual research problem.

5.2 Raster- and grid-based analysis modules

The module *opalsCell* is a raster based analysis tool accumulating specific features (min, max, mean, etc.) of a selected point attribute (z, amplitude, echo width, etc.). Within the presented work the module is used to extract a sub data set (e.g. highest echoes within a raster cell of 0.5 m cell size) and to derive raster maps such as the DSM_{max} and the EW image.

The *opalsGrid* module is a grid-based interpolation tool to derive digital surface or terrain models (DSM/DTM) in regular grid structure using simple interpolation techniques like moving least squares, nearest neighbor or moving average. In this study the moving least squares interpolation with a plane as functional model, i.e., a tilted regression plane is fitted through the k-nearest neighbors (k), is used to derive DSM_{mls} and σ_z.

The module *opalsAlgebra* can be employed to derive grid or raster models by combining multiple input grid and/or raster data sets. The cell values are calculated by applying an algebraic formula based on the values of the respective input raster images and/or grids. Any mathematical formula, and even an entire program code returning a scalar value, can be passed. For the current work this module is applied for calculating the combined DSM, nDSM and the classification images.

5.3 Echo Ratio module

The aim of *opalsEchoRatio* is to derive the slope adaptive echo ratio (sER) for all (or at least selected) points of an OPALS Data Manager (ODM). The results are stored as an additional attribute for each point in the ODM. To derive raster images or grids of the sER the modules opalsCell or opalsGrid respectively can be applied. For the current test sites sER grid modules were derived using the opalsGrid module.

5.4 Morphological module

The *opalsMorph* module is used to perform the morphological operations on the raster datasets to eliminate noise and to smooth the outline of objects. The morphological operations applied in this module are based on binary mathematical morphology. It operates on binary images, which are defined as a set of object (foreground, "1") and non-object (background, "0") elements. Usually the elements are arranged in a regular grid, however, this is not required. Operations use a kernel, or structuring element, which is slid over the image to probe the existence of objects at each locus. The kernels are themselves binary images, i.e., a subset of the grid. The two basic operations are erosion and dilation. The result of the erosion operation is the set of all elements for which the area covered by the kernel, if the kernel is centered on the element, only consists of object elements. The opposite of erosion is dilation, which is defined as the set of all elements which are covered by the kernel if the kernel is centered over an object element. Even though the two operations can be considered to be opposites, they are not inverse in the algebraic sense, i.e. erosion and dilation applied consecutively in general do not yield the original image. It is true, however, that erosion of the inverted image is the same as the inversion of a dilated image and vice versa. Further operations can be defined by combining these basic operators and possibly more general set-theoretic operators as well. For example the opening operation consists of performing erosion and dilation in that order. Opening by a disk shaped kernel rounds convex corners and prunes protrusions extending into the background (smoothing from inside). Closing on the other hand consists of first performing the dilation followed by erosion. If closing by a disk shaped kernel the result is that concave corners are rounded and cracks where the background protrudes into the object are filled. A detailed description of morphological operations can be found in Gonzalez and Woods (1992). The basic kernels are usually symmetric, the concrete shape being tied to the definition of a particular distance function, i.e. the set of all elements within a given radius from the origin. The most common kernels are square, diamond, and circle shaped kernels based on the Chebyshev (chessboard), Manhattan (taxicab), and Euclidian distances respectively. In the *opalsMorph* module the operations (open, close, erode, dilate), kernel shape (diamond, circle, square) and kernel radius can be chosen as parameters. The typical way to implement dilate and erode operations is to first calculate the distance map (Rosenfeld and Pfaltz, 1966) and then apply a threshold depending on the desired kernel size. The distance map is defined as the distance, according to a given distance function, of every background element to the closest foreground element. The algorithm for the computation of the distance map is a two-pass sequential scanning (line sweep) algorithm. The final step is to convert the distance map to a binary image by applying a threshold equal to the kernel radius parameter.

A special joint symposium of ISPRS Technical Commission IV & AutoCarto
in conjunction with
ASPRS/CaGIS 2010 Fall Specialty Conference
November 15-19, 2010 Orlando, Florida

5.5 Vectorization module

The OPALS module *opalsContouring* is used trace the contour of the foreground objects and to export the vectorized contour polygons as ESRI SHAPE files. It uses a linear time labelling algorithm, which avoids the computationally expensive resolution of equivalent labels required by the classical labelling algorithm and has the additional benefit that the desired tracing of the object outline is already an integral part of the algorithm (Chang et al., 2004). The algorithm makes one-pass over the image, but it is not strictly a sequential scanning algorithm. It starts by scanning the image for foreground elements. If a foreground pixel is found, which has not been previously labelled, then the scan is interrupted to follow the contour of the object until the original pixel is again reached. The scan is then resumed from that position. During the contour tracing all the pixels of the contour are labelled with the next unassigned label and the polygon consisting of the outer edges of outlining pixels is stored. During the scanning phase any foreground pixel neighbouring an already labelled pixel gets the label of its neighbour. Since the complete contour of the object has already been traced it is guaranteed that the entire object is assigned the same label and a resolution of equivalent labels is not needed. If a previously unlabelled foreground pixel is found, the tracing is again started with the next unassigned label. As a final result of this operation a raster image consisting of zero and non-zero values is generated, where all the foreground objects are numbered: one object of contiguous pixels have the same pixel values. The highest value of the image equals the number of foreground objects. The holes (background pixels in the foreground object) are handled as inner rings (see ESRI, 1998). Isolated pixels are not traced. Neither are isolated foreground pixels labelled as objects, nor background pixels within objects are treated as holes. Finally there is an option to exclude polygons with an area less than a predefined minimal area from being written to the SHAPE file.

6. RESULTS AND DISCUSSION

For each test sites the nDSM, the EW, the sER and the σ_z-image was calculated using the above described OPALS modules. For the classification of building and vegetation areas *opalsAlgebra* was used. A hierarchic classification scheme was applied meaning, that in a first step the building areas and in a second step the vegetation areas were derived. Based on empirical analyses, thresholds for all input data were found which are summarized in Tab. 1. For the differentiation between vegetation and buildings the surface roughness information (i.e. σ_z- and EW-image) was used. As can be seen in Fig. 2b and 2c, the EW-image is better suited for surface roughness determination within dense tree crowns and building borders than the σ_z-image. Thus, the σ_z-information was not used for classifying the vegetation areas. The derived building and vegetation polygons (Fig. 2d) have a high quality and even small single trees are properly delineated.
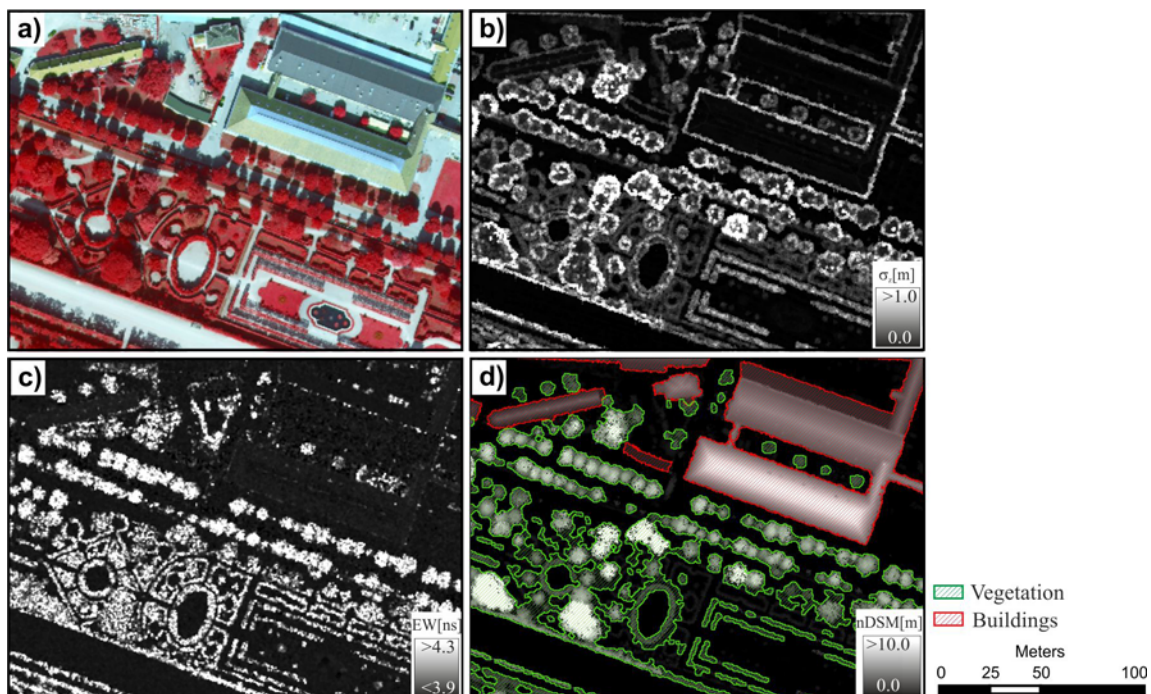

Figure 2. Results of a subset of the *Schönbrunn* test site. (a) Orthophoto, (b) σ_z- image, (c) EW-image, (d) nDSM superimposed with the derived building and vegetation polygons. All images have a spatial resolution of 0.5 m. The minimum mapping unit for buildings was 15 m² and 5 m² for vegetation.

A special joint symposium of ISPRS Technical Commission IV & AutoCarto
in conjunction with
ASPRS/CaGIS 2010 Fall Specialty Conference
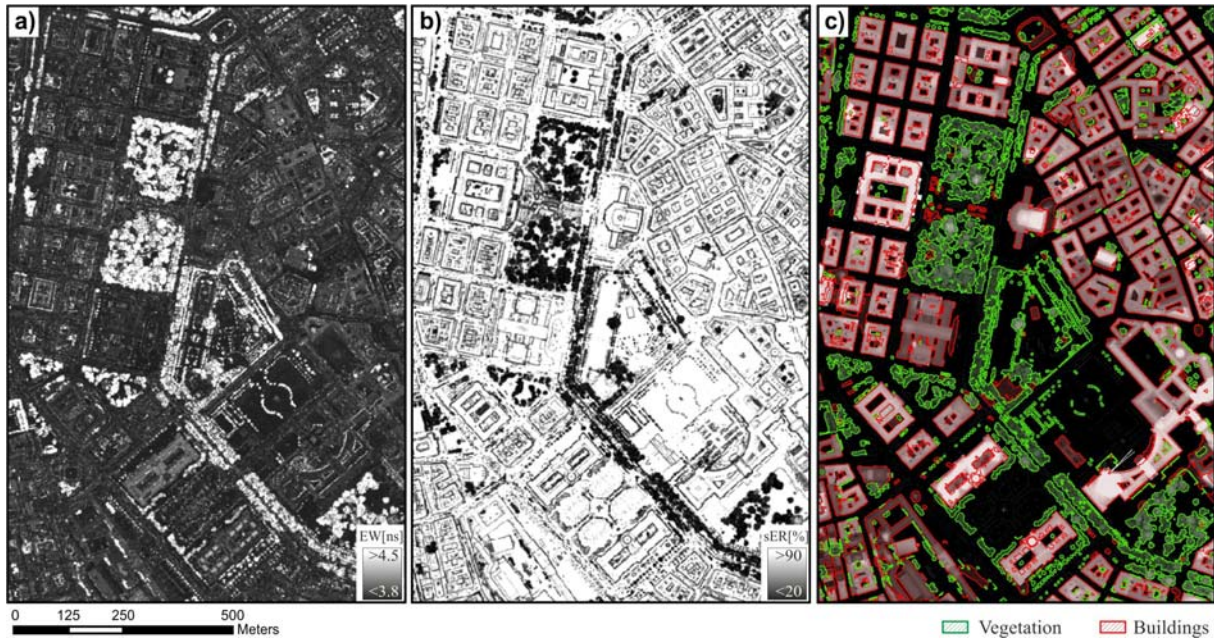November 15-19, 2010 Orlando, Florida

Figure 3. Results of the test site *city centre*. (a) EW- image, (b) sER-image, (c) nDSM superimposed with the derived building and vegetation polygons. All images have a spatial resolution of 0.5 m. The minimum mapping unit for building and vegetation polygons was 15 m².

Table 1. Knowledge-based decision-tree for deriving building and vegetation areas from full-waveform LiDAR data.

Land cover	nDSM [m]	EW [ns]	σ_z [m]	sER [%]	
Building	≥ 2.0	< 4.2	≤ 0.5	≥ 60.0	---
Vegetation	≥ 2.0	> 4.1	---	≤ 60.0	!= building

In general, the sER is a suitable quantity for differentiating penetrable from non-penetrable surfaces. As can be seen in Fig. 3b the buildings roofs in the test site *city centre* appear often as penetrable surfaces due to roof gardens, chimneys, antennas, satellite dishes, balustrades, different height levels for sub-roof areas, etc. Consequently, the overlapping range of sER values between buildings and vegetation increases. However, the derived miss-classifications, which often occur along building borders, can be removed by using morphologic operations (i.e. opening and closing). For a more detailed modeling of roofs three-dimensional (3D) approaches for building extraction, reconstruction and regularization are required as for example published in Dorninger and Pfeifer (2008). As such 3D approaches are computing- and time-intensive, the derived building classification can be used to limit the 3D point cloud analyses only on the potential building regions, which makes such approaches applicable for large areas in an economic way.

7. CONCLUSION

In this paper a workflow for deriving building and vegetation outlines from full-waveform LiDAR data was presented. The applied software modules are implemented into the scientific software system OPALS. The scripting possibility of the OPALS modules allows an efficient and reliable classification of full-waveform LiDAR data in an operational manner. The derived GIS-ready building and vegetation polygons can be used for a series of applications and have shown the high potential as well as the additional benefit of full-waveform LiDAR data for land cover classifications.

REFERENCES

Chang, F., Chen, C.-J. and Lu, C.-J., 2004. A Linear-Time Component-Labeling Algorithm Using Contour Tracing Technique. *Computer Vision and Image Understanding*, 93, 206-220.

Dorninger, P. and Pfeifer, N., 2008. A Comprehensive Automated 3D Approach for Building Extraction, Reconstruction, and Regularization from Airborne Laser Scanning Point Clouds. *Sensors*, 8(11), 7323-7343.

ESRI, 1998. ESRI Shapefile technical description. http://www.esri.com/library/whitepapers/pdfs/shapefile.pdf. Retrieved 2007-07-04.

Gonzalez, R.C. and Woods, R.E., 1992. *Digital Image Processing*, 3rd edition. Addison-Wesley Pub (SD)

A special joint symposium of ISPRS Technical Commission IV & AutoCarto
in conjunction with
ASPRS/CaGIS 2010 Fall Specialty Conference
November 15-19, 2010 Orlando, Florida

Haala, N. and Walter, V., 1999. Automatic Classification of Urban Environments for Database Revision using LIDAR and Color Aerial Imagery. In: *International Archives of Photogrammetry and Remote Sensing, 3-4 June, 1999*, Valladolid, Spain, Vol. Vol. 32, Part 7-4-3 W6: 7.

Höfle, B., Mücke, W., Dutter, M., Rutzinger, M. and Dorninger, P., 2009. Detection of building regions using airborne LiDAR – A new combination of raster and point cloud based GIS methods. *GI_Forum 2009 - International Conference on Applied Geoinformatics, Salzburg*, 66-75.

Hollaus, M. and Höfle, B., 2010. Terrain roughness parameters from full-waveform airborne LiDAR data. In: W. Wagner and B. Székely (Editors), ISPRS TC VII Symposium - 100 Years ISPRS, Vienna, Austria, 287-292.

Hollaus, M., Mandlburger, G., Pfeifer, N. and Mücke, W., 2010. Land cover dependent derivation of digital surface models from airborne laser scanning data. *International Archives of Photogrammetry, Remote Sensing and the Spatial Information Sciences. PCV 2010, Paris, France.*, Vol. 39(3), 6.

Mandlburger, G., Otepka, J., Karel, W., Wagner, W. and Pfeifer, N., 2009. Orientation And Processing Of Airborne Laser Scanning Data (opals) - Concept And First Results Of A Comprehensive Als Software. In: *ISPRS Workshop Laserscanning `09*, Paris, Vol. IAPRS, Vol. XXXVIII, Part 3/W8: 55-60.

Miller, R.B. and Small, C., 2003. Cities from space: potential applications of remote sensing in urban environment research and policy. *Environmental Science & Policy*, 6, 129-137.

OPALS, 2010. OPALS - Orientation and Processing of Airborne Laser Scanning Data, http://www.ipf.tuwien.ac.at/opals/. Last accessed June 2010.

Rosenfeld, A. and Pfaltz, J., 1966. Sequential operations in digital picture processing. *J. ACM*, 13(4), 471-494.
Rottensteiner, F., Trinder, J., Clode, S. and Kubik, K., 2005. Using the Dempster-Shafer Method for the Fusion of LIDAR Data and Multi-spectral Images for Building Detection. *Information Fusion*, 6(4), 283-300.

Rutzinger, M., Höfle, B., Hollaus, M. and Pfeifer, N., 2008. Object-Based Point Cloud Analysis of Full-Waveform Airborne Laser Scanning Data for Urban Vegetation Classification. *Sensors*, 8, 4505-4528.

Scop++, 2010. SCOP++ - Programpackage for Digital Terrain Models, http://www.ipf.tuwien.ac.at/products; http://www.inpho.de. Last accessed June 2010.

Wagner, W., Ullrich, A., Ducic, V., Melzer, T. and Studnicka, N., 2006. Gaussian decomposition and calibration of a novel small-footprint full-waveform digitising airborne laser scanner. *ISPRS Journal of Photogrammetry & Remote Sensing*, 60(2), 100-112.

A special joint symposium of ISPRS Technical Commission IV & AutoCarto
in conjunction with
ASPRS/CaGIS 2010 Fall Specialty Conference
November 15-19, 2010 Orlando, Florida